JHR 86: 19–45 (2021)
doi: 10.3897/jhr.86.71225
https://jhr.pensoft.net

RESEARCH ARTICLE

JOURNAL OF Hymenoptera RESEARCH
A peer-reviewed open-access journal
The International Society of Hymenopterists

Stars in subtropical Japan: a new gregarious *Meteorus* species (Hymenoptera, Braconidae, Euphorinae) constructs enigmatic star-shaped pendulous communal cocoons

Shunpei Fujie[1], So Shimizu[2,3], Koichi Tone[4], Kazunori Matsuo[5], Kaoru Maeto[2]

1 *Osaka Museum of Natural History, Nagaikoen 1–23, Higashisumiyoshi, Osaka 546–0034, Japan* **2** *Laboratory of Insect Biodiversity and Ecosystem Science, Graduate School of Agricultural Science, Kobe University, Rokkodaicho 1–1, Nada, Kobe, Hyogo 657–8501, Japan* **3** *Research Fellow (DC1), Japan Society for the Promotion of Science, Tokyo, Japan* **4** *Okinawa Municipal Museum, Uechi 2–19–6, Okinawa 904–0031, Japan* **5** *Faculty of Social and Cultural Studies, Kyushu University, Motooka 744, Nishi, Fukuoka 819–0395, Japan*

Corresponding author: Shunpei Fujie (shunpei.fujie@gmail.com)

Academic editor: Jose Fernandez-Triana | Received 20 July 2021 | Accepted 3 October 2021 | Published 29 October 2021

http://zoobank.org/4C11898D-A5A4-44BD-89C2-D049E6B991B4

Citation: Fujie S, Shimizu S, Tone K, Matsuo K, Maeto K (2021) Stars in subtropical Japan: a new gregarious *Meteorus* species (Hymenoptera, Braconidae, Euphorinae) constructs enigmatic star-shaped pendulous communal cocoons. Journal of Hymenoptera Research 86: 19–45. https://doi.org/10.3897/jhr.86.71225

Abstract

A new gregarious braconid parasitoid wasp of Euphorinae, *Meteorus stellatus* Fujie, Shimizu & Maeto **sp. nov.**, is described from the Ryukyu Islands in Japan, based on an integrative taxonomic framework. The phylogenetic position of the new species within the Meteorini was analyzed based on DNA fragments of the mitochondrial cytochrome c oxidase 1 (CO1) and the nuclear 28S rDNA genes. The new species was recovered as a member of the *versicolor* complex of the *versicolor* + *rubens* subclade within the *pulchricornis* clade. The new species is a gregarious parasitoid of two *Macroglossum* species (Lepidoptera: Sphingidae) and constructs single or several unique star-shaped cocoon masses separately suspended by very long threads. The evolution of gregariousness and spherical cocoon masses is discussed.

Keywords

Endoparasitoid, female-biased sex ratio, integrative taxonomy, Lepidoptera, *Macroglossum*, phylogeny, species delimitation, Sphingidae

Introduction

The pupae of parasitoid wasps cannot actively escape various risks, such as predation, parasitism, pathogenesis, and environmental stresses. Therefore, cocoons and mummies play important roles in protecting soft and exarate pupae from such risks (Gauld and Bolton 1988; Shaw and Huddleston 1991; Maeto 2018).

Members of Braconidae, one of the most diverse hymenopteran families, form various types of cocoons and mummies to adapt to various natural enemies and environmental threats. Many gregarious braconids produce communal cocoon masses, while discrete cocoons for each individual are also constructed (Shaw and Huddleston 1991). Final-instar braconid larvae emerge from host organisms and then spin a cocoon using silk from the labial glands (e.g., Shaw and Huddleston 1991; Quicke 2015). In some gregarious species, wasp larvae not only spin individual cocoons but also cooperate to construct massive communal cocoons (Zitani and Shaw 2002).

The cosmopolitan braconid genus *Meteorus* Haliday consists of more than 300 valid species (Yu et al. 2016). As the genus *Zele* Curtis is apparently nested within the *Meteorus* species tree, *Meteorus* is a paraphyletic group and its rearrangement into several monophyletic genera is pending (Maeto 1990b; Stigenberg and Ronquist 2011). Maeto (1990b) has divided the *Meteorus* species into seven morphologically and biologically defined species groups, while monophyly has been supported partially (Stigenberg and Ronquist 2011).

Meteorus species are solitary or gregarious koinobiont endoparasitoids of Lepidoptera or Coleoptera larvae (Huddleston 1980; Stigenberg and Ronquist 2011; Maeto 2018). Their cocoons are either suspended (pendulous) or not, and the cocoon suspension is one of diagnostic characters to identify the *pulchricornis* group (Maeto 1989a). The gregarious species construct either independent (e.g., *M. acerbiavorus* Belokobylskij, Stigenberg & Vikberg, *M. heliophilus* Fischer, and *M. rubens* Nees) or communal cocoons (e.g., *M. congregatus* Muesebeck, *M. komensis* Wilkinson, *M. kurokoi* Maeto, and *M. townsendi* Muesebeck) (Maeto 1989b; Zitani and Shaw 2002; Zitani 2003; Stigenberg et al. 2011). The latest molecular phylogeny has suggested that the gregariousness is a derived character in the *pulchricornis* + *rubens* group complex (Stibenberg and Ronquist 2011). So far, six types of cocoon architectures have been observed in the gregarious species of *Meteorus*, as is shown in Table 1. However, the evolution of gregariousness and cocoon architectures within the genus *Meteorus* has been poorly studied, and more bionomical and phylogenetic information is thus needed.

Although the cocoon structure of *Meteorus* is quite mysterious, larval behavior associated with cocoon formation has received little attention, with only a few reports examining it (Askari et al. 1977; Zitani and Shaw 2002; Maeto 2018). Recently, unique star-shaped cocoon masses of an undescribed gregarious species of *Meteorus* have been observed in subtropical Japan (Mitamura 2013). Therefore, this study aims to describe that gregarious species of *Meteorus* based on integrative morphological and molecular evidence and observe its cocoon-mass formation behavior. The phylogenetic position of the new species and evolution of gregariousness and cocoon masses are also discussed.

Table 1. The types of cocoon masses in gregarious *Meteorus*.

Types	Characteristics	Species	References
A	loosely clumped within a host pupal chamber	**Palearctic species**	
		M. acerbiavorus	Stigenberg et al. 2011.
		M. heliophilus	Maeto 1990a
		M. rubens	Maeto 1990a
B	individually suspended from host plant by a thread	**Neotropical species**	
		M. oviedoi	Shaw and Nishida 2005
		M. papiliovorus	Zitani and Shaw 2002
C	sparsely arranged and suspended by a common cable	**Palearctic species**	
		M. kurokoi	Maeto 1989b
		Neotropical species	
		M. restionis	Barrantes et al. 2011
D	loosely clumped and suspended by a common cable	**Neotropical species**	
		M. cecavorum	Aguirre and Shaw 2014
		M. juliae	Aguirre and Shaw 2014
E	congregated and directly attached to host plant without a cable	**Neotropical species**	
		M. congregatus	Zitani and Shaw 2002
F	communal and suspended by a common cable	**Afrotropical species**	
		M. komensis	Zitani and Shaw 2002
		Neotropical species	
		M. townsendi	Zitani and Shaw 2002
		undescribed species	Sobczak et al. 2012
		Oriental species	
		M. stellatus sp. nov.	Present study

Materials and methods

Study fields

The field collection of host moth larvae to observe the cocoon formation behavior of emerged larvae of wasps was conducted at Okinawa Municipal Museum, Okinawa City, Okinawa-hontô, Okinawa Prefecture, Japan. Some materials were also collected within Okinawa-hontô (Okinawa Prefecture) and Amami-ôshima (Kagoshima Prefecture), Japan. All materials were from the middle part of the Ryukyu Islands, the subtropical Oriental region in Japan.

Morphological observation and terms

Morphological observation was conducted with a stereoscopic microscope (SMZ800N, Nikon, Tokyo, Japan). Specimens and cocoons were photographed using a Digital Microscope (VHX-1000, Keyence, Osaka, Japan) with a 10–130× lens. Multi-focus photographs were stacked in the software associated with the Keyence System. Multi-focus photographs of cocoon masses were taken using a single lens reflex camera (α7II, Sony, Tokyo, Japan) with a micro-lens (A FE 50 mm F2.8 Macro SEL50M28, Sony). The RAW format photographs were developed using Adobe Lightroom CC v.2.2.1 (Adobe Systems Inc., San Jose, CA, USA), and stacked using Zerene Stacker v.1.04 (Zerene Systems LLC., Richland, WA, USA). The holotype of *M. komensis*, deposited in the Natural History Museum, London, UK was also examined by the second author

using a stereoscopic microscope (SMZ1500, Nikon). Multi-focus photographs were taken using an α7II camera with micro-lenses (LAOWA 25 mm F2.8 2.5–5× ULTRA MACRO, Anhui Changgeng Optics Technology Co., Ltd, Hefei, China). The captured RAW format photographs were developed and stacked as per the aforementioned photo technique used for the cocoon masses. The figures were edited in Microsoft PowerPoint 2019.

The description style mostly follows that of Stigenberg and Ronquist (2011). The morphological terms and measurements follow those of Richards (1977) and van Achterberg (1988). The following abbreviations are used: **OOL** = ocelli-ocular line, **OD** = ocelli diameter of a posterior ocellus, and **POL** = posterior ocellar line.

The abbreviations for repositories are listed below:

CNC Canadian National Collection of Insects, Ottawa, Canada;
ELKU Entomological Laboratory, Faculty of Agriculture, Kyushu University, Fukuoka, Japan;
EMUS Utah State University Insect Collection (= American Entomological Institute: AEI), Department of Biology, Utah State University, Logan, Utah, USA;
EUM Ehime University Museum, Matsuyama, Japan;
KPMNH Kanagawa Prefectural Museum of Natural History, Odawara, Japan;
MNHA Museum of Nature and Human Activities, Sanda, Japan;
NARO Institute for Agro-Environmental Sciences, NARO (= NIAES: National Institute for Agro-Environmental Sciences), Tsukuba, Japan;
NHMUK Natural History Museum, London, United Kingdom (formerly BMNH);
NSMT National Museum of Nature and Science, Tsukuba, Japan;
OMM Okinawa Municipal Museum, Okinawa, Japan;
OMNH Osaka Museum of Natural History, Osaka, Japan;
RUM Ryukyu University Museum, Okinawa, Japan;
SEHU the Laboratory of Systematic Entomology, Faculty of Agriculture, Hokkaido University, Sapporo, Japan;
TARI Taiwan Agricultural Research Institute Council of Agriculture, Executive Yuan, Taichung, Taiwan;
ZISP Zoological Institute, Russian Academy of Sciences, St Petersburg, Russia.

Secondary sex ratio

To investigate the secondary sex ratio of wasps, the number of males and females of all enclosed wasps that emerged from each host larva was counted for 11 host larvae (Suppl. material 1: Table S1). Cocoon masses with hyper-parasitoids were excluded, and the number of dead cocoons was not counted. The effect of the number of total wasps on the proportion of males was analyzed using a generalized linear model (GLM). A logit link function and binomial error distribution were employed. The mean proportion of males was estimated from the average number of total wasps. The analysis was performed in IBM SPSS Statistics for Windows, v. 25.0 (IBM Corp., Armonk, NY, USA).

Observation of cocoon formation behavior

The cocoon formation behavior of wasp larvae was observed at a laboratory of OMM, in June 2019 by the third author. It was recorded with video cameras (Sony Handycam, HDR-CX470 and HDR-XR150, Sony). The suspended larvae were blown with air currents created by breathing, as there was no wind, which would enhance the merging of each individually suspended larva in the laboratory as it would in natural conditions. A single silk thread spun by an individual larva is called a "thread", and intertwined threads are called a "cable" as in Barrantes et al. (2011). A short movie showing the cocoon formation behavior is available on YouTube (https://www.youtube.com/watch?v=AuHarLHolPM).

Molecular analysis

Gene selection

To delimit a species, fragments of a mitochondrial protein encoding gene, cytochrome c oxidase 1 (CO1), were selected, because its evolutionary rate is more or less rapid and it is one of the most common genes used for population to species level phylogenetic analysis (this is well-known as the DNA barcoding gene). To infer the phylogenetic relationships among species of Meteorini (*Meteorus* and *Zele*), CO1 and a nuclear noncoding gene, 28S rRNA (28S), were selected. 28S is a gene that has evolved more slowly than CO1 and is usually used for species-groups or higher-level phylogeny; therefore, the combined CO1 and 28S analysis can provide a higher resolution of species phylogeny.

Taxon sampling and outgroups

A total of 44 species of *Meteorus* including five morphospecies were sampled as ingroups. Five species of *Zele* were also sampled as ingroups because *Zele* is deeply nested within the *Meteorus* tree (Stigenberg and Ronquist 2011). Three species from different tribes of euphorine genera were sampled as outgroups (*Syrrhizus* Förster, *Syntretus* Förster, and *Peristenus* Förster). A total of 177 sequences of CO1 and 172 of 28S were compiled from GenBank. Sequences obtained from databases sometimes contain unreliable information (e.g., Klimov et al. 2019; Shimizu et al. 2020), and an evaluation of such sequences is always strongly recommended to ensure that the analysis is accurate. In the present study, the sequences used by Stigenberg and Ronquist (2011) and several additional sequences were considered as reliable sources. The complete information of the sampled taxa and sequences is available in the Suppl. material 2: Table S2.

DNA extraction, amplification, and sequencing

Table 2. Primer information for PCR.

Target	Primer name	Sequence (5' to 3')	References
CO1	CO1 lco hym	CAA ATC ATA AAG ATA TTG G	Schulmeister (2003)
	CO1 hco extB*	CCT ATT GAW ARA ACA TAR TGA AAA TG	Schulmeister (2003)
28S	28SD1F	ACC CGC TGA ATT TAA GCA TAT	Harry et al. (1997)
	28SD5R*	CCC ACA GCG CCA GTT CTG CTT ACC	Schulmeister (2003)

The newly collected samples from Okinawa were stored in 99.9% ethanol for DNA extraction. DNA was extracted from a right mid or/and hind leg. The protocols followed from PCR to sequencing were according to the work of Shimizu et al. (2020), except for the primers in Table 2, for which the PCR conditions were as follows: CO1: initial denaturation (2'00") at 95 °C, 35 cycles of denaturation (0'30") at 95 °C, annealing (0'30") at 48 °C, an extension (1'00") at 72 °C, and a final extension (10'00") at 72 °C; 28S: 1'00" at 95 °C, 40 cycles of 0'30" at 95 °C, 0'30" at 48 °C, 1'30" at 72 °C, and 5'00" at 72 °C.

Species delimitation

Partial fragments of CO1 were used for species delineation. A total of 189 sequences were used for analysis (Suppl. material 2: Table S2). To obtain an accurate multiple sequence alignment (MSA), MSA was conducted using MEGA v.10.0.5 (Kumar et al. 2018) based on amino acids. First, the codon positions of all nucleotide sequences were adjusted, the nucleotide sequences were translated to amino acids, the amino acid sequences were aligned by CLUSTAL W (Thompson et al. 1994) implemented in MEGA with default settings, the amino acid alignment was checked by eye, and finally the aligned amino acid sequences were retranslated to nucleotides. The final dataset was 657 bp without indels.

To delimit the species, both distance- and topology-based methods were employed as below. Using both methods, three types of datasets were analyzed: (1) *Meteorus* + *Zele* + outgroups, (2) *Meteorus* + *Zele*, and (3) *Meteorus*. Prior to the analysis, identical haplotypes were removed from the datasets on the web server of ALTER (Glez-Peña et al. 2010) (available at: http://sing.ei.uvigo.es/ALTER/).

Distance-based method (ABGD)

The barcoding gap based analysis, Automatic Barcode Gap Discovery (ABGD) (Puillandre et al. 2012), was ran on the graphic web version of ABGD (available at: http://wwwabi.snv.jussieu.fr/public/abgd/abgdweb.html), with the following parameters: Pmin = 0.001, Pmax = 0.1, Steps = 10, X (relative gap width) = 1.0, model = Kimura (K80) (TS / TV = 2.0), and Nb bins (for distance distribution) = 20.

Topology-based method (GMYC)

The General Mixed Yule Coalescent (GMYC) analysis was employed. GMYC analysis requires an ultrametric tree (UTree) as an input. To construct the UTree, the model and parameters was selected on a web server of the smart model selection (SMS) (Lefort et al.

2017) (available at: http://www.atgc-montpellier.fr/phyml-sms/): the GTR+G+I model was selected as the best fit model under the Bayesian information criterion (BIC). The UTree was generated using BEAST v.2.6.3 (Bouckaert et al. 2019), with a random starting tree, the uncorrelated lognormal relaxed clock model, and the coalescent tree prior. A Bayesian Markov chain Monte Carlo (MCMC) was run for 40,000,000 generations, with trees sampled every 5,000 generations, and a burnin of anterior 25%. The convergence of run was assessed using Tracer v.1.6 (Rambaut and Drummond 2007): run reached a stationary distribution and all effective sample sizes (ESS) were greater than 200. A majority-rule consensus ultrametric tree was finally generated using TreeAnnotator v.2.6.3 (Bouckaert et al. 2019). GMYC analysis was run using the GMYC function of the R-package Splits (Fujisawa and Barraclough 2013) (available at: http://r-forge.r-project.org/projects/splits/) using R v.3.6.3 (R Core Development Team 2020).

Phylogenetic analysis

The phylogeny of Meteorini species was inferred with both the Bayesian Inference (BI) and maximum likelihood (ML) approaches using a concatenated CO1 and 28S fragments.

MSA

Although the MSA of CO1 was already performed in the species delimitation, MSA for 28S was conducted in the MAFFT online service (Katoh et al. 2019), using the Q-INS-i algorithm, which is the structural alignment method for RNA (Katoh and Toh 2008; Katoh and Standley 2013). Ambiguously aligned regions were automatically removed from the dataset using trimAl v.1.2 (Capella-Gutíerrez et al. 2009), with default parameters. The final datasets were 657 (CO1) and 560 (28S) bp in length: the concatenated CO1 and 28S dataset was 1,217 bp.

Terminal species selection

In order to exclude the taxon sampling bias, a single sequence for each species was selected based on the conservative results of the species delimitation analysis by ABGD: sequences of 61 *Meteorus* species, six *Zele* species, and three outgroup species were finally selected (Table 3).

Model selection

Each codon position within the CO1 fragment was treated as a different data block, but not for noncoding 28S. The best-fit substitution model was determined using PartitionFinder v.2.1.1 (Lanfear et al. 2017) with the greedy search algorithm under the corrected Akaike information criterion (AICc): the selected model was the GTR+I+Γ model for the first and second codon position of CO1 and 28S, and GTR+Γ for the third codon position of CO1.

Table 3. Nomenclature systems for Meteorini species. The following abbreviations are used: *pulchri.* = *pulchricornis*.

Species	Present study	Stigenberg et al. (2011)	Maeto (1990)
	clade / subclade / complex	Clade	group / subgroup
Meteorus ictericus A, B	*ictericus* / – / –	I	*ictericus* / –
M. ruficeps	*ictericus* / – / –	I	*ictericus* / –
M. aff. *ruficeps*	*ictericus* / – / –	I	*ictericus* / –
Meteorus sp.	*ictericus* / – / –	–	–
M. artocercus	*pulchri.* / *colon* / –	IIA	–
M. cinctellus	*pulchri.* / *colon* / –	IIA	*pulchri.* / *colon*
M. colon	*pulchri.* / *colon* / –	IIA	*pulchri.* / *colon*
M. stenomastax	*pulchri.* / *colon* / –	IIA	–
M. tenellus A–C	*pulchri.* / *colon* / –	IIA	–
M. pendulus A–C	*pulchri.* / *pendulus* / –	IIB	*pulchri.* / *gyrator*
M. abscissus	*pulchri.* / *pulchri.* / –	IIB	–
M. limbatus	*pulchri.* / *pulchri.* / –	IIB	*pulchri.* / *gyrator*
M. pulchricornis	*pulchri.* / *pulchri.* / –	IIB	*pulchri.* / *pulchri.*
Meteorus sp.	*pulchri.* / *pulchri.* / –	–	–
M. acerbiavorus	*pulchri.* / *rubens-versicolor* / *rubens*	IIB	–
M. rubens A–C	*pulchri.* / *rubens-versicolor* / *rubens*	IIB	*rubens* / –
M. aff. *versicolor* A, B	*pulchri.* / *rubens-versicolor* / *versicolor*	–	*pulchri.* / *versicolor*
M. arizonensis	*pulchri.* / *rubens-versicolor* / *versicolor*	–	–
M. obsoletus	*pulchri.* / *rubens-versicolor* / *versicolor*	IIB	*pulchri.* / *versicolor*
M. tarius	*pulchri.* / *rubens-versicolor* / *versicolor*	–	–
M. stellatus sp. nov.	*pulchri.* / *rubens-versicolor* / *versicolor*	–	–
M. versicolor	*pulchri.* / *rubens-versicolor* / *versicolor*	IIB	*pulchri.* / *versicolor*
M. micropterus	*micropterus* / – / –	IIC	*micropterus* / –
M. abdominator A, B	Unresolved	III	–
M. affinis A–D	Unresolved	III	–
M. cespitator A, B	Unresolved	III	*hirsutipes* / –
M. cis A, B	Unresolved	III	*hirsutipes* / –
M. consimilis	Unresolved	III	–
M. densipilosus	Unresolved	III	–
M. eklundi	Unresolved	III	–
M. filator A, B	Unresolved	III	–
M. gigas	Unresolved	–	–
M. hirsutipes	Unresolved	III	*hirsutipes* / –
M. jaculator	Unresolved	III	–
M. kyushuensis	Unresolved	III	*hirsutipes* / –
M. longicaudis	Unresolved	III	–
M. obfuscatus	Unresolved	III	–
M. aff. *obfuscatus*	Unresolved	III	–
M. oculatus	Unresolved	III	–
M. sibyllae	Unresolved	III	–
Meteorus sp.	Unresolved	–	–
Meteorus sp.	Unresolved	–	–
M. sulcatus	Unresolved	III	*corax* / –
M. tabidus	Unresolved	III	–
M. vexator	Unresolved	III	–
Zela albiditarsus	*Zele*	IV	*Zele* / –
Z. caligatus	*Zele*	IV	*Zele* / –
Z. chlorophthalmus	*Zele*	IV	*Zele* / –
Z. deceptor	*Zele*	IV	*Zele* / –
Z. niveitarsis	*Zele*	–	*Zele* / –
Zela sp.	*Zele*	–	–

Analysis

The BI analyses were conducted using MrBayes v.3.2.2 (Ronquist et al. 2012). A Bayesian MCMC analysis was ran with the following settings: four independent runs, 20

chains each, heating 0.05, random starting trees, and trees sampled every 1,000th generation for 10,000,000 generations. The convergence of the MCMC runs was checked by the average standard deviation of split frequencies (ASDSF) in MrBayes (i.e., ASDSF < 0.01) (Ronquist and Huelsenbeck 2003) and chain stationarity in Tracer v.1.6 (Rambaut and Drummond 2007). Then, we discarded the anterior 25% of the generations as burn-in, obtained estimates for the harmonic means of the likelihood scores from the remaining 75% of the generations using the sump command, and conducted a final check of the convergence of the runs by the value of a potential scale reduction factor (PSRF); if the runs were convergent enough, PSRF was less than 5% divergent from 1.0. Finally, a consensus tree with the Bayesian inference posterior probabilities was obtained using the sumt command in MrBayes. The ML analysis was conducted in IQ-TREE v.2.1.2 (Minh et al. 2020) with a Shimodaira-Hasegawa-like approximate likelihood ratio test (SH-aLRT) (Guindon et al. 2010) and ultrafast likelihood bootstrap replicates (UFBoot2) (Minh et al. 2013; Hoang et al. 2018) for 10,000 replicates. The trees were edited in FigTree v.1.4.3 (Rambaut 2006–2016), Adobe Illustrator CC v.23.0.2, and Photoshop CC v.20.0.4 (Adobe Systems Inc., San Jose, CA, USA).

Results

Species identification

Although the molecular species delimitation was conducted using (1) whole datasets (i.e., *Meteorus* plus *Zele* plus outgroups), (2) *Meteorus* plus *Zele* datasets, and (3) *Meteorus* datasets, the results were congruent among all datasets in both the ABGD and GMYC methods. The number of recognized species was higher in the GMYC than in the ABGD method (Fig. 1). However, all results indicated that *Meteorus stellatus* sp. nov. was a single species.

Baded on morphological data, *M. stellatus* sp. nov. ran to the *versicolor* subgroup of the *pulchricornis* group based on Maeto's (1989a, b) criteria, but it could not be identified as any described species of *Meteorus* (see also Differential diagnosis).

Taxonomic account

***Meteorus stellatus* Fujie, Shimizu & Maeto, sp. nov.**
http://zoobank.org/D8785F79-E874-4854-95D7-5C0A928914CA
[Japanese name: Hoshigata-haraboso-komayubachi]
Figs 2, 3

Etymology. The specific name is a masculine Latin word, "stellatus", meaning "starry", which is derived from the unique shape of the cocoon masses.

Type series. 41♀♀ 40♂♂ (all from Japan). ***Holotype*** ♀ (OMNH): "Japan: Okinawa Is., Okinawa City, Goya / Kitanakagusuku Vil., Shimabukuro, Okinawa Kodomono-kuni, 3. VI. 2019 cocoon masses), K. TONE et al. leg." "9. VI. 2019 emerged".

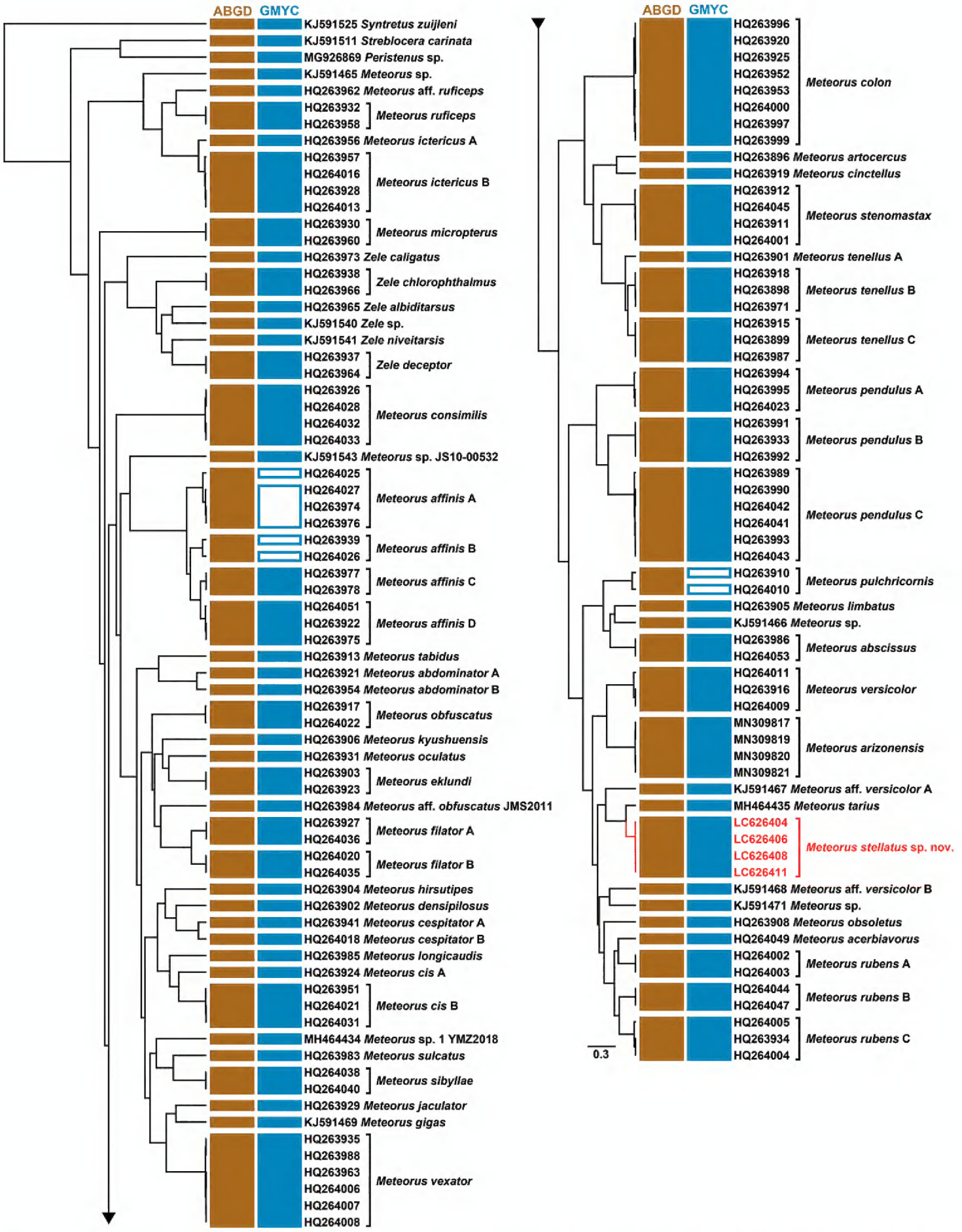

Figure 1. Species delimitation of *Meteorus* plus *Zele* plus closely related outgroups based on ABGD and GMYC methods, shown using a Bayesian consensus ultrametric tree generated using BEAST. Although the species delimitation was conducted using (1) *Meteorus* plus *Zele* plus outgroups, (2) *Meteorus* plus *Zele*, and (3) *Meteorus* sequences or topologies, all results were congruent; therefore, all results are shown as a summarized unit for each method.

***Paratypes*:** 1♀2♂♂ (OMM), same as holotype; 2♀♀2♂♂ (OMM), Okinawa-kodomonokuni, Goya, Okinawa City /Shimabukuro, Kitanakagusuku Vil, Okinawa-hontô Is., collected as cocoon masses on 13.V.2019 and emerged on 19.V.2019, Koichi Tone et. al leg.; 2♀♀2♂♂ (OMNH), Nago City, Okinawa-hontô Is., collected as cocoon masses on *Morinda umbellata* and emerged on 23–24.V.2011, Masashi Sugimoto leg.; 4♀♀4♂♂ (OMNH), Nago City, Okinawa-hontô Is., collected as host larva of *Macroglossum passalus passalus*, and adult wasps emerged on XII.2010 (2♀♀2♂♂) and I.2011 (2♀♀2♂♂), Masashi Sugimoto leg.; 2♀♀2♂♂ (RUM), Hentona, Kunigami Vil., Okinawa-hontô Is., collected as cocoon masses on 14.IV.2011 and emerged on 19.IV.2011, Koichi Sugino leg.; 2♀♀2♂♂ (ZISP), Hentona, Kunigami Vil., Okinawa-hontô Is., collected as cocoon masses on 30.X.2010 and emerged on 7.XI.2010, Kozue Miyagi leg.; 2♀♀2♂♂ (NARO), Aha, Kunigami Vil., Okinawa-hontô Is., collected as cocoon masses on 23.X.2010 and emerged on 25.X.2010, Yasuji Kakazu leg.; 2♀♀2♂♂ (OMNH), Okinawa-kodomonokuni, Goya, Okinawa City, Okinawa-hontô Is., collected as host larva of *Macroglossum pyrrhosticta* feeding *Paederia scandens* on 3.VI.2019, cocoon masses formed on 9.VI.2019, and emerged on 17.VI.2019, Yu Erh Chen leg.; 2♀♀2♂♂ (CNC), Ryukyu University, Nishihara Town, Okinawa-hontô Is., collected as cocoon masses on 22.VI.2005 and emerged on 25–29.VI.2005, Kazuo Minato leg.; 20♀♀20♂♂ (ELKU, EMUS, EUM, KPMNH, MNHA, NHMUK, NSMT, OMM, SEHU and TARI with 2♀♀2♂♂ each), Yoshihara, Chatan Town, Okinawa-hontô Is., collected as cocoon masses on 4.VI.2020 and emerged on 9–11.VI.2020, Tamami Gushiken leg.; 1♀ (OMNH), Chuo-rindo, Amami City, Amami-ôshima Is., 5.VII.2013, Shunpei Fujie leg.

Non-types. 323♀♀228♂♂ adults; 29 cocoon masses (see Suppl. material 1: Table S1).

Distribution. Japan (Ryukyus: Okinawa-hontô Island and Amami-ôshima Island).

Differential diagnosis. *Meteorus stellatus* sp. nov. is most similar to *M. komensis* (Fig. 4) but can be distinguished from the latter by the following combination of characters: the comparatively larger posterior ocelli (in *M. stellatus* sp. nov., OOL/OD = 1.2–1.6, while 1.7 in *M. komensis* (Fig. 4C)), the medially longitudinally strigose first metasomal tergite (Figs 2J, 3F) (fairly striate in *M. komensis*, as is shown in Fig. 4E, F). *Meteorus stellatus* sp. nov. is also very similar to *M. kurokoi* but can be distinguished from *M. kurokoi* by the face width (1.5–1.8× its height in *M. stellatus* sp. nov. (Figs 2E, 3B), while 1.2–1.3× in *M. kurokoi*) and the sculpture of frons (frons with a median longitudinal or a pair of carinae in *M. stellatus* sp. nov. (Fig. 2G), but smooth without any carinae in *M. kurokoi*).

In the key to species of *Meteorus* from the West Palaearctic region (Stigenberg and Ronquist 2011) and China (Chen et al. 2004), *M. stellatus* sp. nov. would run to *M. versicolor* (Wesmael), but can be distinguished from *M. versicolor* by the face width (1.5–1.8× its height in *M. stellatus* sp. nov. (Figs 2E, 3B), while 1.0–1.2× in *M. versicolor*), the sculpture of frons (with a median longitudinal or a pair of carinae in *M. stellatus* sp. nov. (Fig. 2G), but smooth in *M. versicolor*), and the shape of temple (Figs 2C, 3C) (roundly narrowed in *M. stellatus* sp. nov. (Figs 2C, 3C), but directly narrowed in *M. versicolor*).

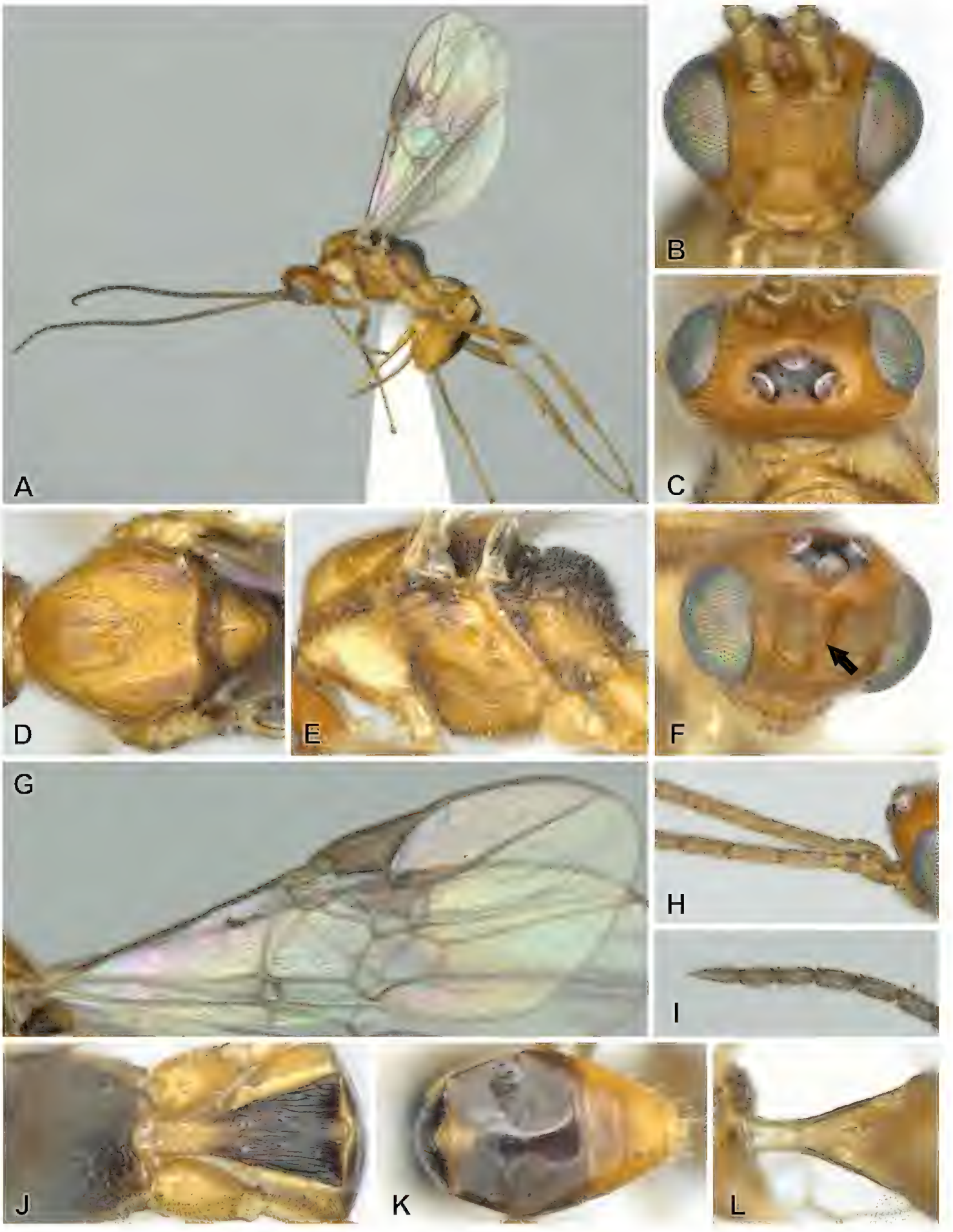

Figure 2. *Meteorus stellatus* sp. nov., ♀ holotype (exceptionally L is a paratype) **A** habitus **B** head, frontal view **C** head, dorsal view **D** mesopleuron and scutellum, dorsal view **E** mesosoma, lateral view **F** head, dorso-lateral view **G** forewing **H** basal antennal segments **I** apical antennal segments **J** propodeum and T1, dorsal view **K** T2 and following tergites, dorsal view **L** T1, ventral view.

The results of a GenBank BLAST search showed that the CO1 sequences of *M. stellatus* sp. nov. were closest to those of *M. arizonensis* Muesebeck and *M. tarius* Huddleston. However, *M. stellatus* sp. nov. can be distinguished from *M. arizonensis*

by its smaller body (the body lengths of *M. stellatus* sp. nov. and *M. arizonensis* are 2.9–3.9 mm and 4.6–5.5 mm, respectively), the longer malar space (the malar space length 1.0–1.4× the basal mandibular width in *M. stellatus* sp. nov. whereas 0.6–0.7× in *M. arizonensis*), the shorter ovipositor sheaths (the ovipositor sheath length 1.1–1.2× length of the first tergite in *M. stellatus* sp. nov. and 1.6–1.9× in *M. arizonensis*); the species can be distinguished from *M. tarius* by its broader face (the face width 1.5–1.7× its height in *M. stellatus* sp. nov. whereas approximately 1.0× in *M. tarius*) and the position of the forewing vein m-cu (slightly antefurcal to interstitial in *M. stellatus* sp. nov., but far antefurcal in *M. tarius*).

Description. Female (holotype; Fig. 2). Body length 3.6 mm.

Head (Fig. 2B, C, F, H, I). Width of head 1.7× median height. Length of eye 1.7× length of temple in dorsal view. Temple roundly narrowed posteriorly. Eyes large and moderately convergent ventrally. Face with width 1.6× height; distinctly and densely transversely striate with fine granulation. Clypeus as wide as face, distinctly separated from face, and punctate-rugose. OOL / OD = 1.2. POL / OD = 1.4. Frons widely smooth, anteriorly with a pair of obscure carinae. Vertex and temple almost smooth. Length of malar space 1.1× basal mandibular width. Antennae with 26 segments; 4th segment 3.1× longer than wide; and penultimate one 1.9× longer than wide.

Mesosoma (Fig. 2D, E, J). Mesosoma length 1.4× height. Mesoscutum entirely covered with short and dense pale setae; median lobe weakly punctulate in anterior 0.6 and mostly rugose reticulate in posterior 0.4; lateral lobes weakly punctulate. Notauli shallow, wide, complete, coarsely rugose-reticulate. Prescutellar depression deep, almost straight, with often five rather fine carinae. Scutellum smooth and distinctly convex. Mesopleuron mostly punctulate, and rugose reticulate anterodorsally. Precoxal sulcus shallow and widely rugose-reticulate. Propodeum entirely coarsely rugose reticulate without median longitudinal carina.

Wings (Fig. 2G). Fore wing with 3.1 mm in length, length of pterostigma 2.9× maximum width, 3-SR / r = 1.2, m-cu distinctly (left) to slightly (right) postfurcal, cu-a far postfurcal, 1-CU1 / cu-a = 0.8. Hind wing with 1M / cu-a = 0.8, 1M / 1r-m = 0.6.

Legs. Tarsal claws with a distinct submedial lobe. Hind leg: outer surface of coxa punctate; femur 4.7× longer than wide, and distinctly and densely punctate.

Metasoma (Fig. 2J, K, L). 1st tergite 1.6× longer than apical width; dorsopes absent; mostly smooth anteriorly, longitudinally strigose with some rugosity medially, densely striate in posterior 0.3; ventral borders jointed from the base of segment to about middle point. Remaining terga smooth. Ovipositor slightly down-curved; length of ovipositor sheath 0.7× C+SC+R, 0.3× fore wing, and 1.2× 1st tergite.

Color (Fig. 2A). Brownish yellow, except for following parts infuscate: stemmaticum, apical segments of antennae, dorsal part of propleuron, side of scutellum, metanotum, propodeum, apex of hind femur and tibia, posterior half of 1st tergite, 2nd tergite (often except for anteromedially), 3rd tergite and ovipositor sheath; and palpi pale yellow. Wing membrane hyaline; pterostigma light brown, faintly paler basally.

Variation. Body length 2.9–3.9 mm. Width of head 1.6–1.8× median height. Length of eye 1.5–1.7× length of temple in dorsal view. Face with width 1.5–1.7× height. OOL / OD = 1.2–1.6. POL / OD = 1.3–1.7. Frons with a longitudinal carina

Figure 3. *Meteorus stellatus* sp. nov., ♂ paratype **A** habitus **B** head, frontal view **C** head and mesonotum, dorsal view **D** basal antennal segments **E** apical antennal segments **F** propodeum and T1, dorsal view **G** T2 and following tergites, dorsal view.

or a pair of obscure carinae. Length of malar space 1.0–1.4× basal mandibular width. Antennae with 26–31 segments; 4th segment 2.9–3.6× longer than wide; and penultimate one 1.7–2.0× longer than wide. Mesosoma length 1.4–1.5× height. Fore wing length 2.7–3.5 mm with length of pterostigma 2.8–3.3× maximum width, 3-SR / r = 0.8–1.4, m-cu distinctly postfurcal to interstitial, 1-CU1 / cu-a = 0.6–1.1. Hind wing with 1M / cu-a = 0.6–1.0, 1M / 1r-m = 0.5–0.7. Hind femur 4.6–4.9× longer than wide. 1st metasomal tergite 1.5–1.8× longer than apical width; longitudinally strigose with often some rugosity medially; length of ovipositor sheath 0.6–0.8× C+SC+R and

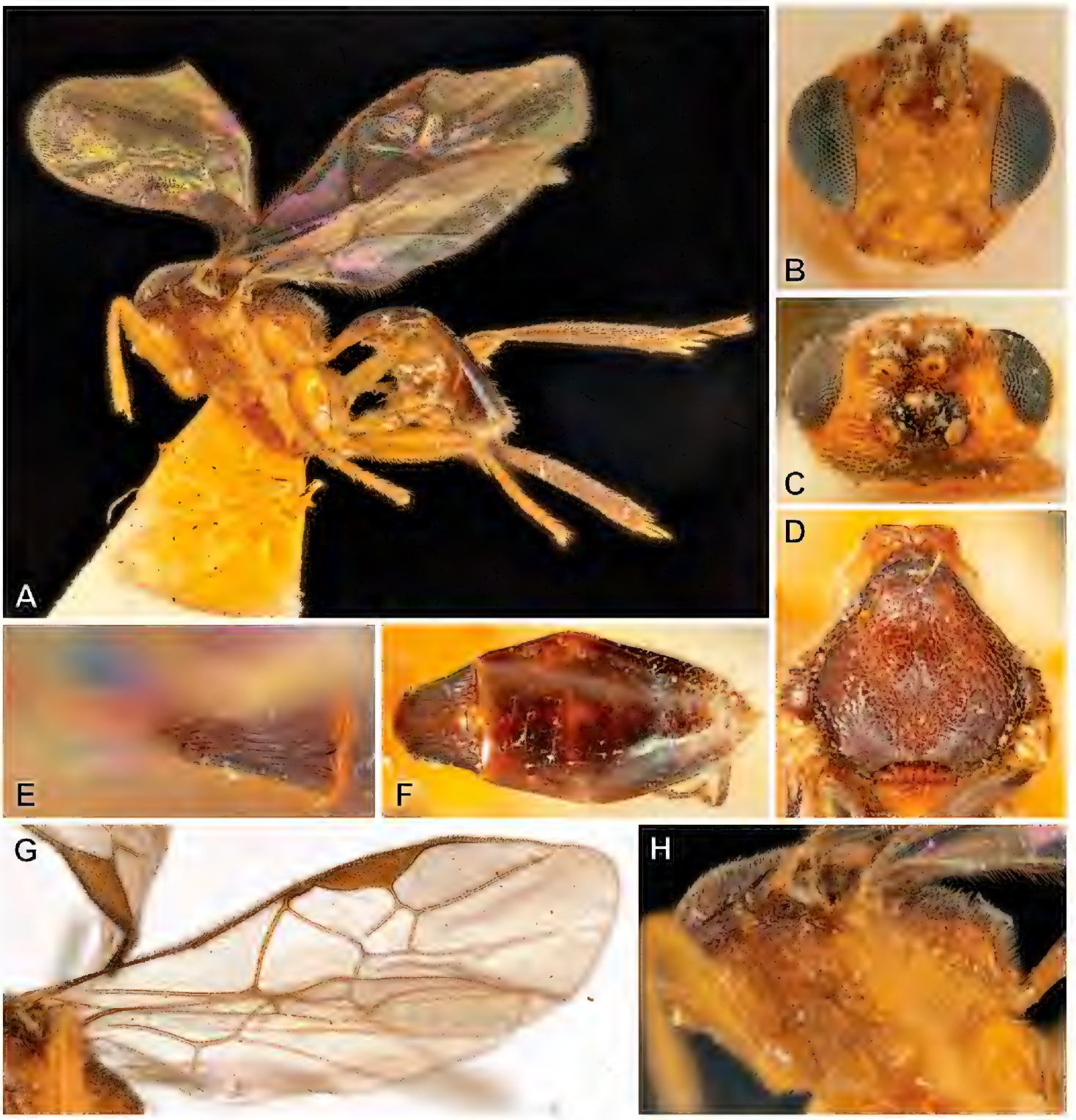

Figure 4. *Meteorus komensis* Wilkinson, ♀ holotype **A** habitus **B** head, frontal view **C** head, dorsal view **D** mesoscutum, dorso-lateral view **E** T1, dorsal view **F** T2 and following tergites, dorsal view **G** forewing **H** mesosoma, lateral view.

1.1–1.2× 1st tergite. 2nd tergite brownish yellow to infuscate anteromedially. Pterostigma unicolored or faintly paler basally.

Males (Fig. 3). Similar to females, except for length of eye 1.6–1.9× length of temple in dorsal view; width of face 1.6–1.8× height; OOL / OD = 1.1–1.4; POL / OD = 1.4–1.8; length of malar space 1.1–1.7× basal mandibular width; antennae with 27–31 segments; penultimate segments of antenna 2.2–2.8× longer than wide; hind femur 4.6–5.1× longer than wide; 1st metasomal tergite 1.6–1.9× long than apical width; propleuron not darkened dorsally.

Hosts and host plants. Two species of Sphingidae (Lepidoptera) were identified as hosts of *M. stellatus* sp. nov.: *Macroglossum passalus* (Drury) feeding on

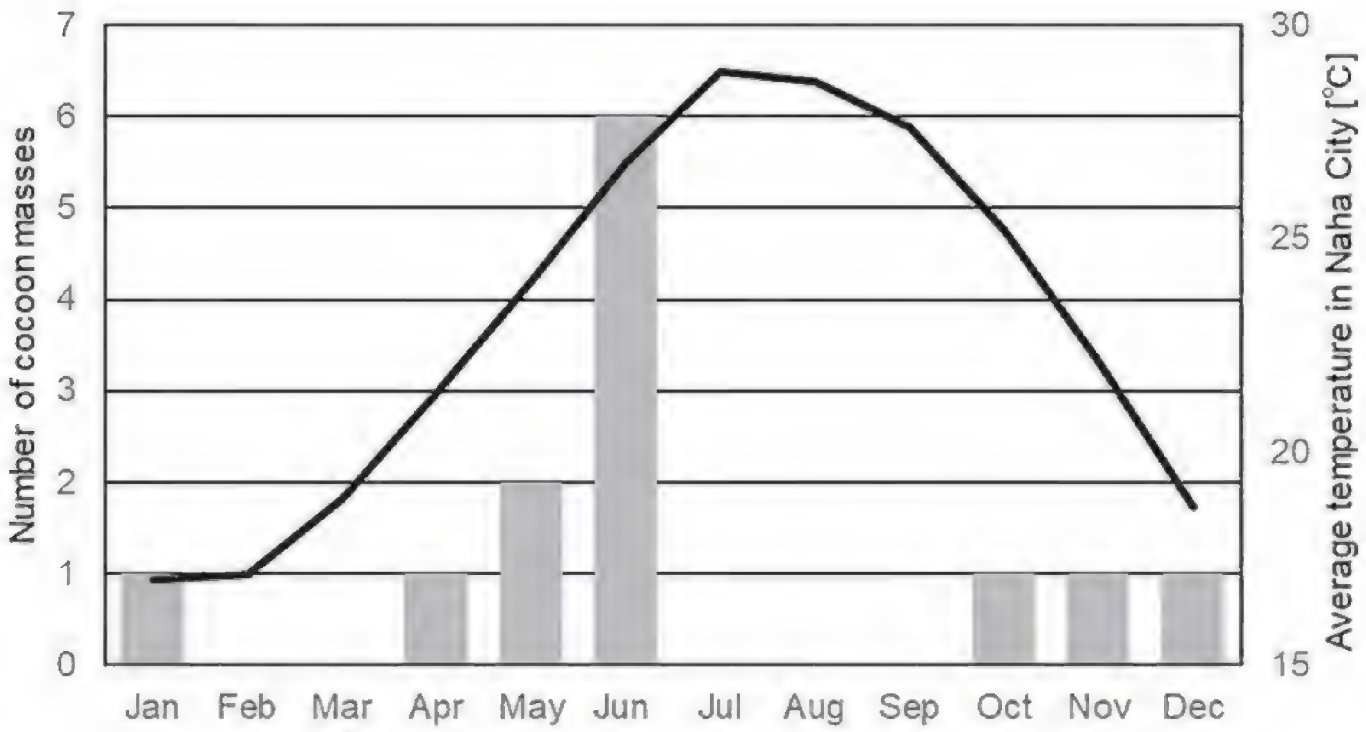

Figure 5. Seasonal changes in the adult emergence of *Meteorus stellatus* sp. nov. (bars indicating the number of cocoon masses) and in the monthly average temperature in Naha City, Okinawa-hontô Island (a solid line).

Daphniphyllum glaucescens Blume (Daphniphyllaceae) and *M. pyrrhosticta* Butler feeding on *Paederia foetida* Linnaeus [= *P. scandens* (Lour.) Merr.] (Rubiaceae). All wasp larvae of *M. stellatus* sp. nov. emerged from mature larvae of the host sphingids.

Hyper-parasitoids. Some hymenopteran hyper-parasitoids emerged from the cocoon masses after the emergence of *M. stellatus* sp. nov. adults. The following three species were identified as morphospecies at the generic level: *Tetrastichus* sp. (Eulophidae), *Eurytoma* sp. (Eurytomidae), and *Aphanogmus* sp. (Ceraphronidae) (Suppl. material 2: Table S2).

Habitats. Despite the multiple field collection sessions at primary forest areas in the Okinawa-hontô and Amami-ôshima Islands, only one specimen of *M. stellatus* sp. nov. was sampled from a secondary evergreen forest in the latter island. Most other specimens of *M. stellatus* sp. nov. were collected from a campus of the University of the Ryukyus, urban parks, and back yards in Okinawa-hontô Island, by finding suspended cocoon masses or rearing host larvae. As the host sphingids and their host plants are abundant in or around the edges of sparse forests, *M. stellatus* sp. nov. likely prefers rather open forests.

Phenology. The emergence of adult wasps occurred from April to June and from October to January, but not during the hottest season from July to September (Fig. 5).

Secondary sex ratio. The proportion of males (secondary sex ratio) ranged from 0.20 to 0.64, showing a gradual increase with the total number of wasps per host larva (Fig. 6). The positive effect of the total number of wasps on the sexual ratio was significant (B = 0.010, Wald Chi-Square = 18.129, df = 1, $p < 0.001$). The estimated mean of the proportion of males was 0.36 (95% confidence interval = 0.31–0.42, significantly less than 0.50) in the average number of total wasps (50.5), indicating an overall female-biased sex ratio.

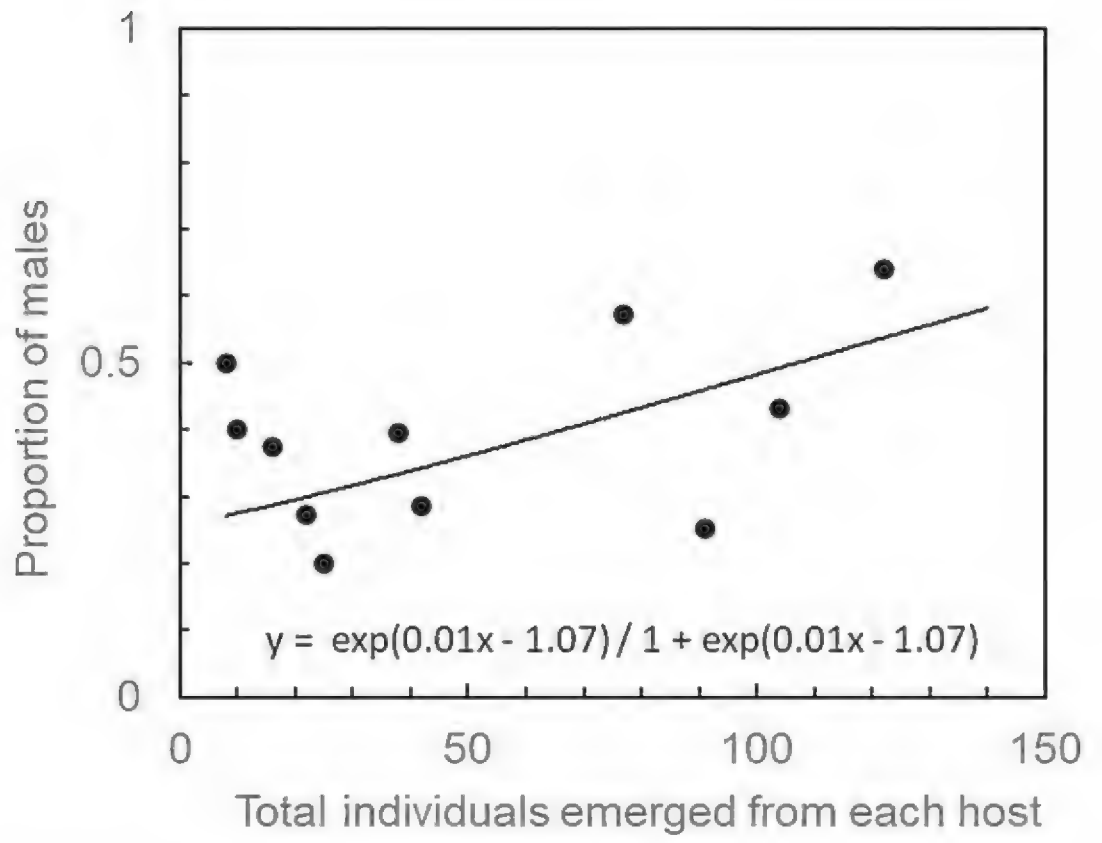

Figure 6. Sex ratios of emerged adults of *Meteorus stellatus* sp. nov. in relation to the number of individuals per host larva.

Cocoon mass formation. The third author observed a case of larval emergence and subsequent cocoon formation in the laboratory. At approximately 1:30 p.m. on June 9, 2019, approximately 100 larvae of *M. stellatus* sp. nov. emerged from the abdomen of a matured larva of *M. pyrrhosticta* on the vine of *P. foetida* by chewing holes (Fig. 7A). The larvae commenced hanging down from the host plant substance with their own suspensory threads as soon as they emerged (Fig. 7B). The larvae began to cluster by actively rotating, twisting, swaying, and horizontally stretching (Fig. 7C). When the larvae found the threads of other individuals, they actively went down, intertwined with said threads, and eventually merged together. Once they formed a large mass, the mass did not descend any more (Fig. 7D). In rare cases, several larvae moved from the upper mass to the lower mass as the cable of the former intertwined with that of the latter, owing to the blowing wind. No further larval transfer was observed after approximately 70 min of the emergence of the larvae. Initially, the shape of the larval masses was irregular (Fig. 7E), but gradually the larvae adopted a spherical shape (Fig. 7F, G). The larvae twisted their upper bodies and spun the thread at the posterior of their body, namely inside the cocoon mass. The silk walling action lasted approximately 40 min, along with the spinning of their own individual cocoons (Fig. 7H, I). Finally, three cocoon masses were completed approximately 2 h after larval emergence (Fig. 7J). A video of the entire process of cocoon mass formation is available at the following address: https://www.youtube.com/watch?v=AuHarLHolPM.

The host sphingid died on the following day after wondering. The color of the cocoons gradually darkened over a few days. After 8 days, 68 females and 23 males of *M. stellatus* sp. nov. emerged from these three cocoon masses. The wasps emerged simultaneously, cutting the tip of each cocoon.

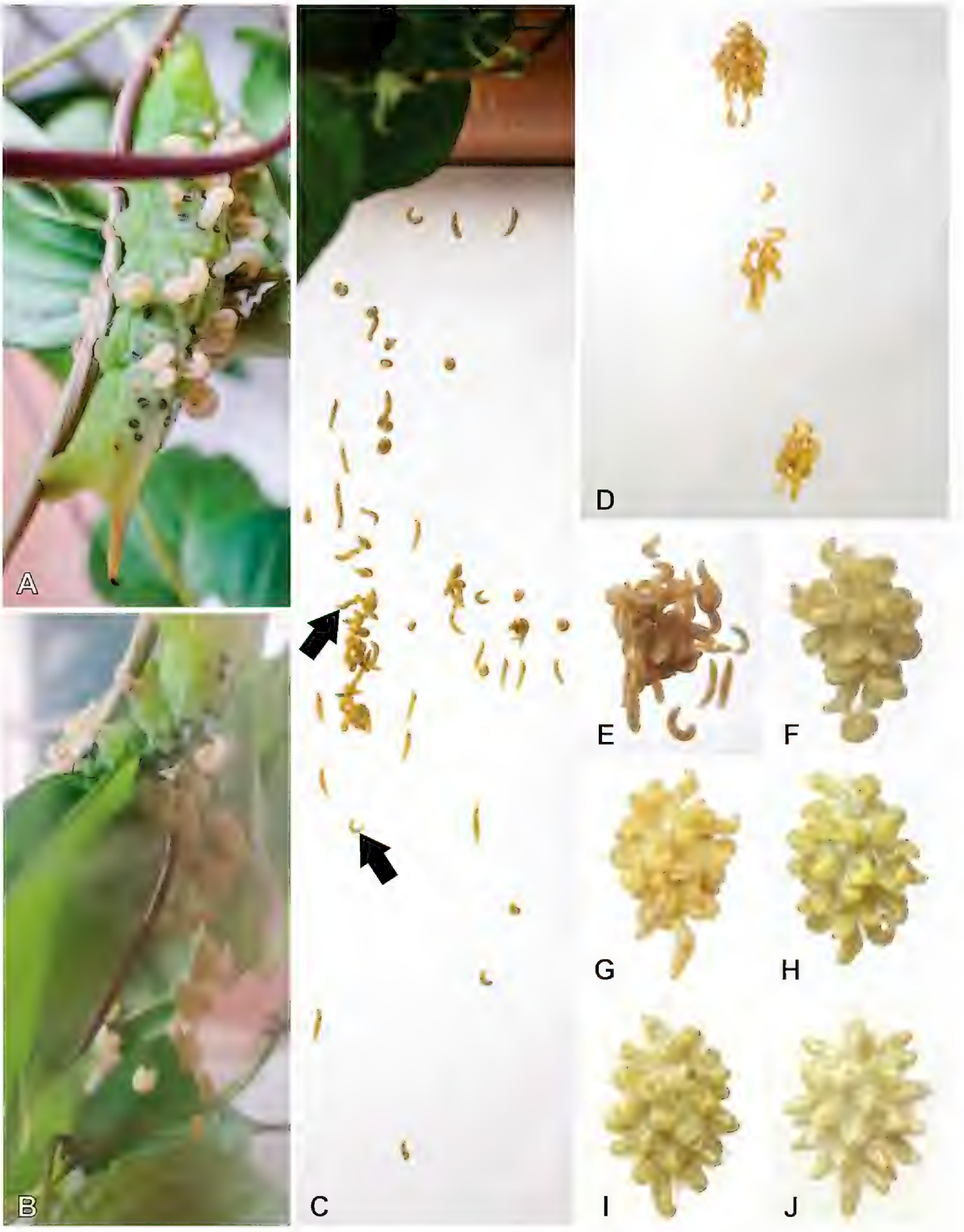

Figure 7. Cocoon forming behavior of *Meteorus stellatus* sp. nov. **A** emerging from a host larva (start time) **B** hanging down from the host plant substance (2 min) **C** intertwining with threads: arrows show larvae looking for other threads (39 min) **D** almost merging into three masses (57 min) **E–J** forming spherical cocoon masses (**E** 30 min **F** 65 min **G** 69 min **H** 84 min **I** 105 min **J** 139 min).

Characteristics of the cocoon masses. The cocoon masses of *M. stellatus* sp. nov. (Fig. 8) were light brown to brown, 7–14 mm in width, 9–23 mm in length, and regularly spherical to ovoid with minimally 12 (Fig. 8D) to maximally over 100 cocoons

(Fig. 8C). Exceptionally, approximately 200 cocoons formed a collapsed large mass in an artificial breeding case (Fig. 8B). Each cocoon mass was suspended by a single thick cable. The cable was 12–100 cm in length. Although most larvae constructed such cocoon masses, sometimes a few single larvae formed their own cocoons on the cable (Fig. 8F). The cable consisted of individual threads, which were tightly intertwined, like a rope (Fig. 8G). The anterior third to half of individual cocoons was exposed outward and fairly distributed on the spherical or ovoid surface. The posterior half of individual cocoons was invisible under the dense silk wall. Adults emerged by opening an anterior outside cocoon cap, which was circular shaped and tapering (Fig. 8F). Cocoons with such a regular cap are typical of the *pulchricornis* clade of *Meteorus* (Askari et al. 1977; Maeto 1989a, b, 1990a).

Phylogeny of Meteorini and affinity of *M. stellatus* sp. nov. The Meteorini phylogeny is illustrated in Fig. 9. The Meteorini classification was also revised based on our phylogeny and those of Maeto (1990b) and Stigenberg et al. (2011) (Table 3). Although our topology was poorly resolved at the species level, it was mostly congruent with that of Stigenberg and Ronquist (2011). Meteorini was recovered as a monophyletic group. Meteorini species were divided into five clades (Fig. 9; Table 3). *Zele* was recovered as a robustly supported monophyletic clade and nested within *Meteorus* species. Monophyly was robustly supported for the *ictericus* and *pulchricornis* clades but not for the unresolved clade. The *pulchricornis* clade was divided into four internal subclades (the *colon*, *pendulus*, *pulchricornis*, and *rubens* subclades).

Meteorus stellatus sp. nov. was recovered as an ingroup of the *versicolor* complex of the *rubens* subclade within the *pulchricornis* clade and sister to *M. tarius*.

Discussion

Our observation of *M. stellatus* sp. nov. shows that gregarious cocoon masses were constructed by the highly elaborated cooperation of larvae. The larvae never merged immediately after emergence from their host, but initially just descended. This seems to reinforce the idea that the suspended cocoon makes the pupating wasp inaccessible to some potential enemies (Shaw and Huddleston 1991; Quicke et al. 2006; Zitani 2003; Shirai and Maeto 2009; Maeto 2018). It seems that predators, like ants, seldom encounter suspended larvae because the threads of larvae are attached to the plant subtract only by a small area.

The cable of gregarious *Meteorus* is thought to be very resistant to breaking and highly tolerant to environmental stress (Barrantes et al. 2011). A cable of *M. stellatus* sp. nov. consists of a lot of individual threads and seems to be very strong, pretty much like that of *M. restionis* Shaw & Jones (Barrantes et al. 2011). Interestingly, cocoon masses of *M. townsendi* are suspended by a fairly long cable, the length of which is approximately 3.0 m (Zitani and Shaw 2002; Zitani 2003), while the longest cable of *M. stellatus* sp. nov. is approximately 1.0 m. According to our observation, the long individual threads and the adequate wind during the hanging period seem to make it easier for the larvae of *M. stellatus* sp. nov. to merge with each other. The larvae continue to spin thread until they are able to merge into a cocoon mass, and in most cases, they never go down unnecessarily after that.

Figure 8. Cocoon masses of *Meteorus stellatus* sp. nov. **A** habitus, medium-sized **B** habitus, exceptionally large-sized and somewhat collapsed in an artificial condition **C** a medium-sized cocoon mass **D, E** small-sized cocoon masses **F** independent cocoons near a cocoon mass **G** a part of suspending thread, consisting of individual cable.

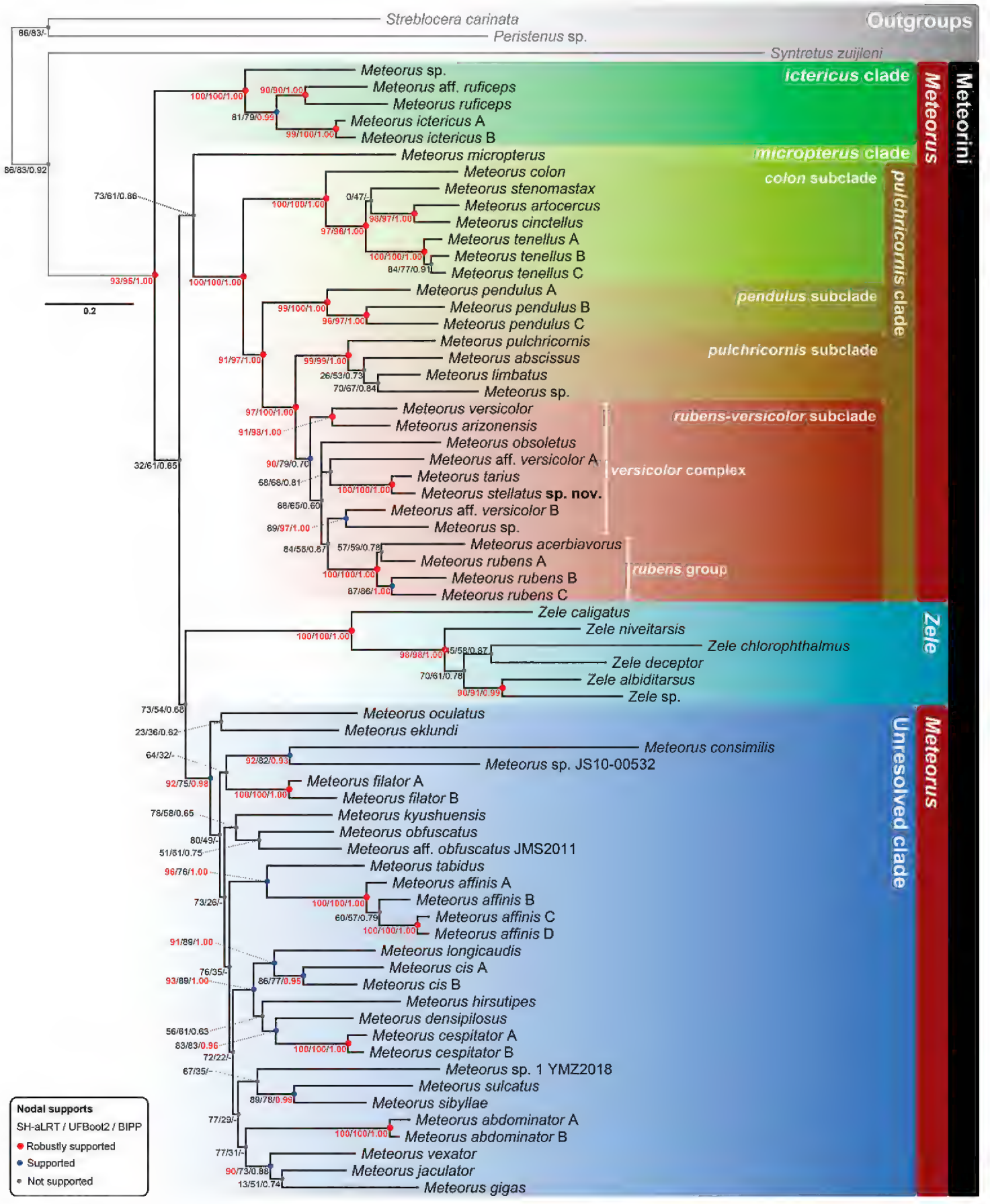

Figure 9. Maximum likelihood tree of Meteorini generated using IQ-TREE (BIPP, Bayesian inference posterior probabilities; SH-aLRT, a Shimodaira-Hasegawa-like approximate likelihood ratio test; UF-Boot2, ultrafast likelihood bootstrap replicates).

The star-shaped cocoon masses of *M. stellatus* sp. nov. can reduce the risk of hyperparasitism, because the exposed area of each individual cocoon is apparently smaller than the solitary cocoon or non-star-shaped cocoon masses, as suggested by the spherical cocoons of *M. komensis* (Zitani 2003). The outer cocoons of non-circular cocoon masses of gregarious *Cotesia glomerata* (Linnaeus) (Braconidae, Microgastrinae) are actually more easily parasitized than the inner ones (Tagawa and Fukushima 1993;

Tanaka and Ohsaki 2006). Therefore, the evolution of gregariousness and spherical cocoon masses seems reasonable.

The sex ratio has been studied in gregarious species of *Meteorus*, while a similar pattern of female-biased sex ratio has been shown in *Macrostomion sumatranum* (Enderlein) (Braconidae, Rogadinae), which is also a gregarious parasitoid of matured sphingid larvae (Maeto and Arakaki 2005). Both in the gregarious parasitoid category, the number of wasps emerged from each host varies widely (8–122 in *M. stellatus* sp. nov. and 26–160 in *Ma. sumatranum*) and the proportion of males increases with it. The female-biased sex ratio could be a result of the local mate competition, as expected in inbreeding gregarious parasitoids (Hamilton 1967; Godfray 1994; Smart and Mayhew 2009), in which the increase of the male proportion may be caused by the oviposition of multiple females on a single host larva (Werren 1983). This prediction will be tested by the examination of mating systems, oviposition behavior, and primary sex ratio.

The *pulchricornis* and *rubens* species-groups belong to the monophyletic lineage of *pulchricornis* clade (Fig. 10), in which both solitary and gregarious species are included and cocoons are usually suspended by a spun thread (Maeto 1990b; Stigenberg and Ronquist 2011). It is thus likely that communal cocoon masses of type F have evolved through individually or sparsely suspended gregarious cocoons of type B and C, and subsequently loosely clumped and suspended gregarious cocoons of type D, from suspended solitary cocoons within the *versicolor* complex. However, the evolutionary pathways are not yet clarified because only a few gre-

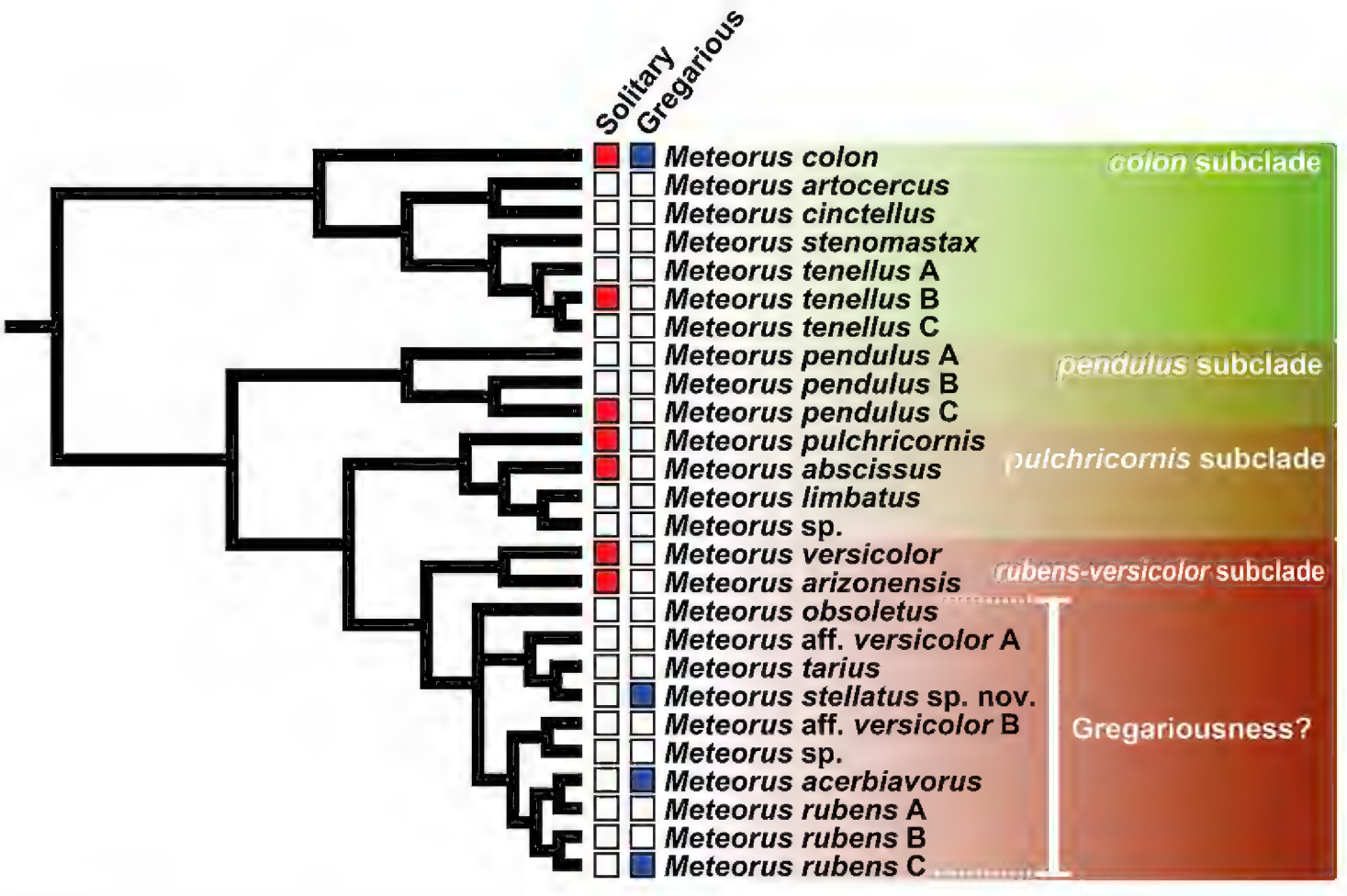

Figure 10. Phylogenetic relationships among the species of *pulchricornis* clade and their lifestyle.

garious species are placed in the present phylogram. Further and comprehensive analyses including more gregarious species are necessary to confirm and expand this evolutionary scenario.

Acknowledgements

We are grateful to Yu Erh Chen, Tamami Gushiken, Kazuo Minato, Toshimasa Mitamura, Kozue Miyagi, Masashi Sugimoto, Koichi Sugino, Nakatada Wachi, Masako Yafuso, and research volunteers of Okinawa Zoo and Museum for collecting and offering the materials; to Kota Sakagami for identifying the host sphingid; to Kees van Achterberg and Jose Fernandez-Triana for variable suggestions on the manuscript; to Gavin Broad (NHMUK) for supporting at NHMUK.

This research is partially supported by the Grants-in-Aid for JSPS KAKENHI (Grant numbers 19H00942) to KM and the Grant-in-Aid for JSPS Fellows (Grant Number 18J20333) to SS from the Japan Society for the Promotion of Science. The JSPS Overseas Challenge Program for Young Researchers enabled SS to carry out research at NHMUK.

References

Aguirre H, Shaw SR (2014) Neotropical species of *Meteorus* Haliday (Hymenoptera: Braconidae: Meteorinae) parasitizing Arctiinae (Lepidoptera: Noctuoidea: Erebidae). Zootaxa 3779: 353–367. https://doi.org/10.11646/zootaxa.3779.3.3

Askari A, Mertins JW, Coppel HC (1977) Developmental biology and immature stages of *Meteorus pulchricornis* in the laboratory. Annals of the Entomological Society of America 70: 655–659. https://doi.org/10.1093/aesa/70.5.655

Barrantes G, Triana E, Shaw SR, Jones GZ (2011) Characteristics of the cocoon and natural history of the gregarious *Meteorus restionis* sp. n. (Hymenoptera, Braconidae, Meteorinae) from Costa Rica. Journal of Hymenoptera Research 20: 9–21. https://doi.org/10.3897/jhr.29.867

Bouckaert R, Vaughan TG, Barido-Sottani J, Duchêne S, Fourment M, Gavryushkina A, Heled J, Jones G, Kühnert D, De Maio N, Matschiner M, Mendes FK, Müller NF, Ogilvie HA, du Plessis L, Popinga A, Rambaut A, Rasmussen D, Siveroni I, Suchard MA, Wu C-H, Xie D, Zhang C, Stadler T, Drummond AJ (2019) BEAST 2.5: An advanced software platform for Bayesian evolutionary analysis. PLoS Computational Biology 15: e1006650. https://doi.org/10.1371/journal.pcbi.1006650

Capella-Gutiérrez S, Silla-Martínez JM, Gabaldón T (2009) trimAl: a tool for automated alignment trimming in large-scale phylogenetic analyses. Bioinformatics 25: 1972–1973. https://doi.org/10.1093/bioinformatics/btp348

Chen X-X, He J-H, Ma Y (2004) Fauna Sinica. Insecta Vol. 37. Hymenoptera. Braconidae (II). Science Press, Beijing, 581 pp.

Fujisawa T, Barraclough TG (2013) Delimiting species using single-locus data and the Generalized Mixed Yule Coalescent approach: a revised method and evaluation on simulated data sets. Systematic Biology 62: 707–724. https://doi.org/10.1093/sysbio/syt033

Gauld ID, Bolton B [Eds] (1988) The Hymenoptera. Oxford University Press, Oxford and The Natural History Museum, London, 332 pp.

Glez-Peña D, Gómez-Blanco D, Reboiro-Jato M, Fdez-Riverola F, Posada D (2010) ALTER: program-oriented format conversion of DNA and protein alignments. Nucleic Acids Research 38: W14–W18. https://doi.org/10.1093/nar/gkq321

Godfray HCJ (1994) Parasitoids: Behavioral and Evolutionary Ecology. Princeton University Press, Princeton, 473 pp. https://doi.org/10.1515/9780691207025

Guindon S, Dufayard JF, Lefort V, Anisimova M, Hordijk W, Gascuel O (2010) New algorithms and methods to estimate maximum-likelihood phylogenies: assessing the performance of PhyML 3.0. Systematic Biology 59: 307–321. https://doi.org/10.1093/sysbio/syq010

Hamilton WD (1967) Extraordinary sex ratios. Science 156: 477–488. https://doi.org/10.1126/science.156.3774.477

Harry M, Solignac M, Lachaise D, (1996) Adaptive radiation in the Afrotropical region of the Paleotropical genus *Lissocephala* (Drosophilidae) on the pantropical genus *Ficus* (Moraceae). Journal of Biogeography 23: 543–552. https://doi.org/10.1111/j.1365-2699.1996.tb00016.x

Hoang DT, Chernomor O, von Haeseler A, Minh BQ, Le SV (2018) UFBoot2: improving the ultrafast bootstrap approximation. Molecular Biology and Evolution 35: 518–522. https://doi.org/10.1093/molbev/msx281

Huddleston T (1980) A revision of the western Palaearctic species of the genus *Meteorus* (Hymenoptera: Braconidae). Bulletin of the British Museum (Natural History), Entomology series 41: 1–58.

Katoh K, Rozewicki J, Yamada KD (2019) MAFFT online service: multiple sequence alignment, interactive sequence choice and visualization. Briefings in Bioinformatics 20: 1160–1166. https://doi.org/10.1093/bib/bbx108

Katoh K, Toh H, (2008) Improved accuracy of multiple ncRNA alignment by incorporating structural information into a MAFFT-based framework. BMC Bioinformatics 9: 212. https://doi.org/10.1186/1471-2105-9-212

Katoh K, Standley DM (2013) MAFFT multiple sequence alignment software version 7: improvements in performance and usability. Molecular Biology and Evolution 30: 772–780. https://doi.org/10.1093/molbev/mst010

Klimov PB, Skoracki M, Bochkov AV (2019) Cox1 barcoding versus multilocus species delimitation: validation of two mite species with contrasting effective population sizes. Parasites Vectors 12: e8. https://doi.org/10.1186/s13071-018-3242-5

Kumar S, Stecher G, Li M, Knyaz C, Tamura K (2018) MEGA X: molecular evolutionary genetics analysis across computing platforms. Molecular Biology and Evolution 35: 1547–1549. https://doi.org/10.1093/molbev/msy096

Lanfear R, Frandsen PB, Wright AM, Senfeld T, Calcott B (2017) PartitionFinder 2: new methods for selecting partitioned models of evolution for molecular and morphological phylogenetic analyses. Molecular Biology and Evolution 34: 772–773. https://doi.org/10.1093/molbev/msw260

Lefort V, Longueville J-E, Gascuel O (2017) SMS: smart model selection in PhyML. Molecular Biology and Evolution 34: 2422–2424. https://doi.org/10.1093/molbev/msx149

Maeto K (1989a) Systematic studies on the tribe Meteorini from Japan (Hymenoptera, Braconide) V. The *pulchricornis* group of the genus *Meteorus* (1). Japanese Journal of Entomology 57: 581–595.

Maeto K (1989b) Systematic studies on the tribe Meteorini (Hymenoptera: Braconidae) from Japan. VI. The *pulchricornis* group of the genus *Meteorus* Haliday (2). Japanese Journal of Entomology 57: 768–777.

Maeto K (1990a) Systematic studies on the tribe Meteorini (Hymenoptera: Braconidae) from Japan. VII. The group of *Meteorus ictericus* and *M. rubens*. Japanese Journal of Entomology 58: 81–94.

Maeto K (1990b) Phylogenetic relationships and host associations of the subfamily Meteorinae Cresson (Hymenoptera, Braconidae). Japanese Journal of Entomology 58: 383–396.

Maeto K (2018) Polyphagous koinobiosis: the biology and biocontrol potential of a braconid endoparasitoid of exophytic caterpillars. Applied Entomology and Zoology 53: 433–446. https://doi.org/10.1007/s13355-018-0581-9

Maeto K, Arakaki N (2005) Gregarious emergence of *Macrostomion sumatranum* (Hymenoptera: Braconidae; Rogadinae) from the mummified, full-grown larvae of *Theretra silhetensis* (Lepidoptera: Sphingidae). Entomological Science 8: 131–132. https://doi.org/10.1111/j.1479-8298.2005.00107.x

Minh BQ, Nguyen MAT, von Haeseler A (2013) Ultrafast approximation for phylogenetic bootstrap. Molecular Biology and Evolution 30: 1188–1195. https://doi.org/10.1093/molbev/mst024

Minh BQ, Schmidt HA, Chernomor O, Schrempf D, Woodhams MD, von Haeseler A, Lanfear R (2020) IQ-TREE 2: new models and efficient methods for phylogenetic inference in the genomic era. Molecular Biology and Evolution 37: 1530–1534. https://doi.org/10.1093/molbev/msaa015

Mitamura T (2013) The Handbook of Japanese Cocoon. Bun-ichi (Tokyo): 1–112. [in Japanese]

Puillandre N, Lambert A, Brouillet S, Achaz G (2012) ABGD, automatic barcode gap discovery for primary species delimitation. Molecular Ecology 21: 1864–1877. https://doi.org/10.1111/j.1365-294X.2011.05239.x

Quicke DLJ (2015) The Braconid and Ichneumonid Parasitoid Wasps. Biology, systematics, evolution and ecology. John Wiley & Sons, Ltd., Hoboken, 681 pp. https://doi.org/10.1002/9781118907085

Quicke DLJ, Mori M, Zaldivar-Riverón A, Laurenne NM, Shaw MR (2006) Suspended mummies in *Aleiodes* species (Hymenoptera: Braconidae: Rogadinae) with descriptions of six new species from western Uganda based largely on DNA sequence data. Journal of Natural History 40: 2663–2680. https://doi.org/10.1080/00222930601121288

R Core Development Team (2020) R: a language and environment for statistical computing. https://www.R-project.org/

Rambaut A (2006–2016) Tree Figure Drawing Tool, version 1.4.3, Institute of Evolutionary Biology, University of Edinburgh. http://tree.bio.ed.ac.uk/software/figtree/

Rambaut A, Drummond AJ (2007) Tracer: MCMC trace analysis tool v1.4.1. http://tree.bio.ed.ac.uk/software/tracer?/

Richards OW (1977) Hymenoptera. Introduction and key to families. Handbooks for the Identification of British Insects, 2nd edn. 6: 1–100.

Ronquist F, Huelsenbeck JP (2003) MrBayes 3: Bayesian phylogenetic inference under mixed models. Bioinformatics 19: 1572–1574. https://doi.org/10.1093/bioinformatics/btg180

Ronquist F, Teslenko M, van der Mark P, Ayres DL, Darling A, Höhna S, Larget B, Liu L, Suchard MA, Huelsenbeck JP (2012) MrBayes 3.2: efficient Bayesian phylogenetic inference and model choice across a large model space. Systematic Biology 61: 539–542. https://doi.org/10.1093/sysbio/sys029

Schulmeister S (2003) Simultaneous analysis of basal Hymenoptera (Insecta): introducing robust-choice sensitivity analysis. Biological Journal of Linnean Society 79: 245–275. https://doi.org/10.1046/j.1095-8312.2003.00233.x

Shaw MR, Huddleston T (1991) Classification and biology of Braconid wasps (Hymenoptera: Braconidae). Handbooks for the Identification of British Insects 7(11): 1–126.

Shaw SR, Nishida K (2005) A new species of gregarious *Meteorus* (Hymenoptera: Braconidae) reared from caterpillars of *Venadicodia caneti* (Lepidoptera: Limacodidae) in Costa Rica. Zootaxa 1028: 49–60. https://doi.org/10.11646/zootaxa.1028.1.4

Shimizu S, Broad GR, Maeto K (2020) Integrative taxonomy and analysis of species richness patterns of nocturnal Darwin wasps of the genus *Enicospilus* Stephens (Hymenoptera, Ichneumonidae, Ophioninae) in Japan. ZooKeys 990: 1–144. https://doi.org/10.3897/zookeys.990.55542

Shirai S, Maeto K (2009) Suspending cocoons to evade ant predation in *Meteorus pulchricornis*, a braconid parasitoid of exposed- living lepidopteran larvae. Entomological Science 12: 107–109. https://doi.org/10.1111/j.1479-8298.2009.00301.x

Sobczak JF, Maia DP, Moura JCMS, Costa VA, Vasconcellos-Neto J (2012) Natural history of interaction between *Meteorus* sp. Haliday, 1835 (Hymenoptera: Braconidae) and its hyperparasitoid *Toxeumella albipes* Girault, 1913 (Hymenoptera: Pteromalidae). Brazilian Journal of Biology 72: 211–214. https://doi.org/10.1590/S1519-69842012000100026

Stigenberg J, Ronquist F (2011) Revision of the Western Palearctic Meteorini (Hymenoptera, Braconidae), with a molecular characterization of hidden Fennoscandian species diversity. Zootaxa 3084: 1–95. https://doi.org/10.11646/zootaxa.3084.1.1

Stigenberg J, Vikberg V, Belokobylskij SA (2011) *Meteorus acerbiavorus* sp. nov. (Hymenoptera, Braconidae), a gregarious parasitoid of *Acerbia alpina* (Quensel) (Lepidoptera, Arctiidae) in North Finland. Journal of Natural History 45: 1275–1294. https://doi.org/10.1080/00222933.2011.552807

Tagawa J, Fukushima H (1993) Effects of host age and cocoon position on attack rate by the hyperparasitoid, *Eurytoma* sp. (Hym.: Eurytomidae), on cocoons of the parasitoid, *Cotesia* (= *Apanteles*) *glomerata* (Hym.: Braconidae). Entomophaga 38: 69–77. https://doi.org/10.1007/BF02373141

Tanaka S, Ohsaki N (2006) Behavioral manipulation of host caterpillars by the primary parasitoid wasp *Cotesia glomerata* (L.) to construct defensive webs against hyperparasitism. Ecological Research 21: 570–577. https://doi.org/10.1007/s11284-006-0153-2

Thompson JD, Higgins DG, Gibson TJ (1994) CLUSTAL W: improving the sensitivity of progressive multiple sequence alignment through sequence weighting, position-specific gap penalties and weight matrix choice. Nucleic Acids Research 22: 4673–4680. https://doi.org/10.1093/nar/22.22.4673

Werren JH (1983) Sex ratio evolution under local mate competition in a parasitic wasp. Evolution 37: 116–124. https://doi.org/10.1111/j.1558-5646.1983.tb05520.x

Yu DSK, van Achterberg C, Horstmann K (2016) Taxapad 2016, Ichneumonoidea 2015 Database on flash-drive. Nepean, Ontario. www.taxapad.com

van Achterberg C (1988) Revision of the subfamily Blacinae Foerster (Hymenoptera, Braconidae). Zoologische Verhandelingen Leiden 249: 1–324.

Zitani NM (2003) The evolution and adaptive significance of silk use in the Meteorinae (Hymenoptera, Braconidae). PHD Thesis. University of Wyoming, Laramie.

Zitani NM, Shaw RS (2002) From *Meteorus* to death star. Variations on a silk thread (Hymenoptera: Braconidae: Meteorinae). American Entomologist 48: 228–235. https://doi.org/10.1093/ae/48.4.228

Supplementary material 1

Table S1

Authors: Shunpei Fujie, So Shimizu, Koichi Tone, Kazunori Matsuo, Kaoru Maeto

Data type: excel (.xslx) file

Explanation note: Table S1. Examined materials *Meteorus stellatus* sp. nov.

Link: https://doi.org/10.3897/jhr.86.71225.suppl1

Supplementary material 2

Table S2

Authors: Shunpei Fujie, So Shimizu, Koichi Tone, Kazunori Matsuo, Kaoru Maeto

Data type: excel (.xslx) file

Explanation note: Table S2. Gene bank accession numbers for the sampled taxa in the analyses.

Link: https://doi.org/10.3897/jhr.86.71225.suppl2